Improvement of cascaded semiconductor optical amplifier gates by using holding light injection

Yu, Jianjun; Jeppesen, Palle

Published in:
Journal of Lightwave Technology

Link to article, DOI:
10.1109/50.923474

Publication date:
2001

Document Version
Publisher's PDF, also known as Version of record

Improvement of Cascaded Semiconductor Optical Amplifier Gates by Using Holding Light Injection

Jianjun Yu and Palle Jeppesen, *Member, IEEE*

***Abstract*—The cascadability of semiconductor optical amplifier (SOA) gates by using holding light injection is numerically and experimentally investigated. Our experimental results show that the signal bit error rate after two cascaded SOA gates will be larger than 10^{-9} without holding light injection; however, 11 SOA gates can be cascaded with holding light injection. The results show that the number of cascaded SOA gates by using holding light injection can be strongly increased.**

***Index Terms*—Holding light injection, numerical simulation, optical network, semiconductor optical amplifiers (SOAs), wavelength division multiplexing (WDM).**

I. Introduction

THE semiconductor optical amplifier (SOA) is a promising candidate for cascaded optical fiber systems and optical gating because of the coverage of the entire fiber transmission window and the possibilities for integration and low cost. The low input power dynamic range and high cross-gain modulation (XGM) induced in multichannel gating due to gain saturation and XGM, respectively [1], [2], have been overcome with the introduction of gain control schemes such as feed-forward, laser gain clamping [3], polarization multiplexing technique (PMT) [4], [5], and holding light injection [6], [7]. Theoretical investigation [3] has shown that a four-channel system at 10 Gb/s cannot be cascaded over three SOAs by using small signal injection, nor over six gain clamping (GC)-SOAs by using laser gain clamping with passive and active distributed Bragg reflector (DBR) regions at 1 dB penalty, mainly due to extinction ratio (ER) degradation for the cascaded SOA gates and limited relaxation frequency for the cascaded GC-SOA gates. In order to overcome the limited relaxation frequency of GC-SOA with laser gain control, the methods of holding light injection and PMT can be used. However, PMT involves a complex transmitter.

In this paper, we investigate the performance of cascaded SOA gates by using holding light injection. In a single-channel system, the injected holding light increases the SOA stimulated recombination rate, which results in reduced carrier lifetime and improved gain recovery rate. In this way, the extinction ratio can be improved. In a wavelength-division multiplexing (WDM) system, when the total WDM signal power into the SOA is low, the holding light shares more power as compared to when the total signal power is medium, thus reducing the signal power increment in the signal channels with 1 bit. On the other hand; when the total input signal power is high, the holding light will share less power and decrease the signal power reduction in 1 bit. Therefore, the holding light acts as a reservoir to suppress gain fluctuations of WDM signals in the SOAs. Because the holding light is injected from outside of the SOA, it is not affected by the limited relaxation frequency like a GC-SOA. The gain of the signal will be reduced due to the large holding light. Therefore, the method of holding light injection is more suitable for an optical switch in WDM networks than for an in-line amplifier. Comparing the applications of the SOA for an optical gate and an in-line amplifier, there are the following differences: When the SOA is used as an in-line amplifier, the SOA should have not only a large saturation input power but also large gain because a large saturation input power will lead to a large dynamic range, and a large gain can compensate the loss of a long fiber. This paper will show that a long SOA is beneficial for enhancing the SOA gain; however, the long SOA will lead to a small saturation input power. When the SOA is used as an optical gate, a large saturation input power is the main parameter. We will also show that a short SOA gate has large saturation input power.

This paper is divided into six sections. Section II gives the numerical model for the SOA and two kinds of configurations of cascaded SOA gates. In Section III, the numerical model is verified by several experiments. In Section IV, we experimentally and numerically investigate the cascadability of SOA gates for single-channel systems and further verify our numerical model. In Section V, we numerically investigate the cascadability of SOA gates in multichannel systems. Conclusions are given in Section VI.

II. The Model for Numerical Simulation

In order that the carrier dynamics can be studied along the length of the amplifier, the SOA is segmented into a number of smaller sections. Electron-rate equations are then applied to each section of the cavity [8]–[11]

$$\frac{dn_i}{dt} = \frac{I}{qdlw} - \frac{n_i}{\tau_{s_i}} - \sum_{k=1}^{N} \frac{g_{m_{ik}} I_{av_{ik}}}{E_k}. \tag{1}$$

Here i corresponds to the different amplifier sections and k refers to the different optical input beams. n_i is the carrier density in section i; t is the time; I is the drive current; q is the electronic charge; and d, l, and w are thickness, length, and width of the SOA, respectively. τ_{s_i} is the carrier recombination lifetime

Manuscript received July 10, 2000; revised November 30, 2000.

J. Yu was with Research Center COM, Technical University of Denmark, Lyngby DK-2800, Denmark. He is now with Agere Systems, Murray Hill, NJ 07974 USA.

P. Jeppesen is with Research Center COM, Technical University of Denmark, Lyngby DK-2800, Denmark.

Publisher Item Identifier S 0733-8724(01)03637-4.

TABLE I
PARAMETERS OF THE SOA

Parameters	Value
Gain factor, a_1	$2.5\times10^{-20}\ m^2$
Gain factor, a_2	$7.4\times10^{18}\ m^{-3}$
Gain factor, a_3	$3.155\times10^{25}\ m^{-4}$
Gain factor, a_4	$3\times10^{-32} m^4$
Recombination coefficient, A	$1.5\times10^{8}\ s^{-1}$
Recombination coefficient, B	$2.5\times10^{-17}\ m^3 s^{-1}$
Recombination coefficient, C	$9.4\times10^{-41}\ m^6 s^{-1}$
Active layer width, w	$1.2\ \mu m$
Active layer thickness, d	$0.15\ \mu m$
Number of sections	40
Carrier density at transparency, n_0	$1.1\times10^{24}\ m^{-3}$
Internal loss, α	$2000\ m^{-1}$
Confinement factor, Γ	0.6
refractive index, $n_{e,0}$	3.5
Change in refractive index with carrier density, dN/dn	$-1.2\times10^{-26} m^3$
Carrier density at original threshold, N_{th}	$3\times10^{24}\ m^{-3}$

in section i, $g_{m_{ik}}$ is the material gain in section i for input beam k. E_k is the photon energy, and $I_{av_{ik}}$ represents the average light intensity in segment i of the SOA cavity and for beam k. We neglect the facet reflectivity of the SOA in this paper. For $I_{av_{ik}}$, we apply

$$I_{av_{ik}} = I_{\text{input}_{\text{ik}}} \frac{e^{g_i L_i} - 1}{g_i L_i} \tag{2}$$

where $g_i = \Gamma g_{m_i} - \alpha$ is the net gain in section i, Γ the confinement factor, and α the material loss.

The material gain g_{m_i} is approximated by the following expression [9]:

$$g_{m_i} = a_1(n_i - n_0) - a_2(\lambda - \lambda_N)^2 + a_3(\lambda - \lambda_N)^3 \tag{3}$$

where a_2 and a_3 are empirically determined constants. λ_N is the spectral shift, which is expressed by [11]

$$\lambda_N = \lambda_0 - a_4(n_i - n_0). \tag{4}$$

Here n_0 is the carrier density at transparency, $\lambda_0 = 1550$ nm is the peak wavelength at transparency, and a_4 is a constant characterizing the gain-peak shift. For τ_{s_i}, we use

$$\tau_{s_i} = \frac{1}{A + Bn_i + Cn_i^2} \tag{5}$$

where A, B, and C are the conventional constants.

The phase change φ_i in section i including the linear and nonlinear phase is given by [9]

$$\varphi_i = \frac{2\pi L_i}{\lambda_k} n_{e,0} + \Gamma n_{th} \frac{2\pi L_i}{\lambda_k} \frac{dN}{dn} + \frac{2\pi L_i \Gamma (n_i - n_0)}{\lambda_k} \frac{dN}{dn}. \tag{6}$$

L_i is the cavity length of section i, λ_k is the lightwave wavelength of beam k, $n_{e,0}$ is the refractive index, and dN/dn is the change in refractive index with carrier density. The first term on the right-hand side of this equation represents linear phase; the other two terms on the right-hand side represent nonlinear phase. If no fiber is considered, it is unnecessary for us to investigate the phase change in the cascaded SOA gates because only signal intensity is considered in (1) and (2). All parameters of the SOA are shown in Table I.

The amplified spontaneous emissin (ASE) of the SOA is obtained by multiplying the electrical field with the total gain $\sqrt{G_T}$ and by adding to each spectral component of the signal independent noise terms whose real and imaginary parts are independent Gaussian variables with variance $\sigma^2 = N_{sp} h\nu (G_T - 1)\,\Delta\nu/2$. Here N_{sp} accounts for incomplete population inversion ($N_{sp} = 4$ for the SOA in this work [1]), h is the Plank constant, ν is the signal carrier frequency, and $\Delta\nu$ is the bandwidth occupied by each Fourier component of the discrete Fourier spectrum. It means that the noise figure of the SOA is 8 dB: this value is the same as the one measured in our experiment when the holding light is chosen to be

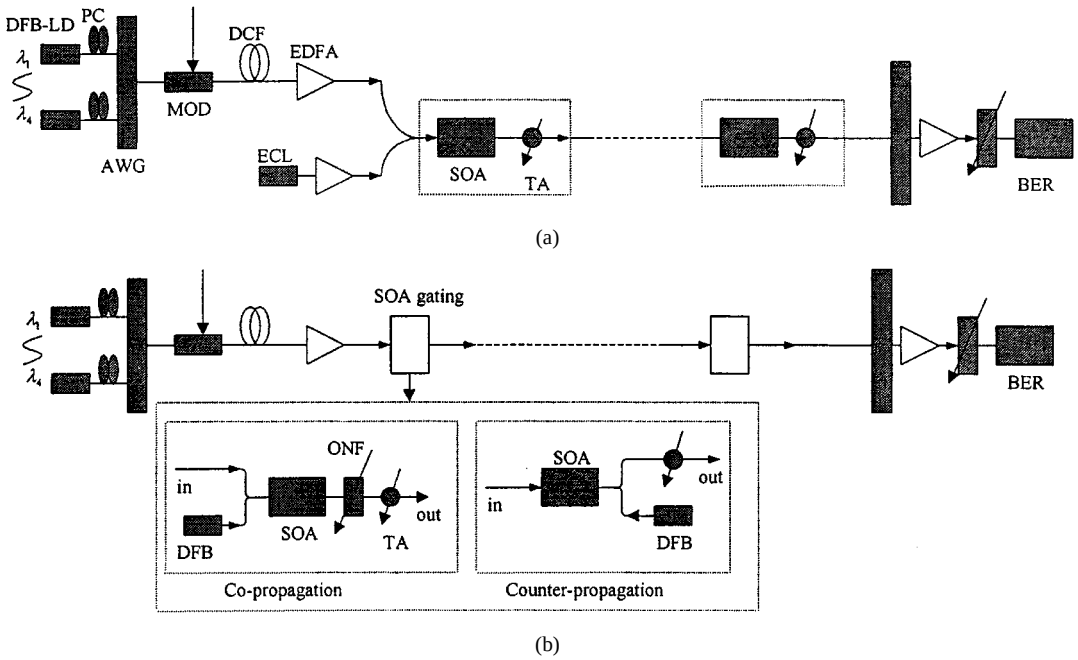

Fig. 1. Two configurations A and B of SOA gating using holding light injection. (a) Configuration A. (b) Configuration B.

about 4 dBm. Reference [1] has shown that there is almost no difference between using this kind of ASE noise model and other complex models of ASE noise.

We consider two SOAs, SOA1 and SOA2, with the same parameters except for the length and injection current. SOA1 is short, with a length of 400 μm operated at 50 or 120 mA. SOA2 is long, with a length of 1200 μm operated at 200 mA, which is the same as the value used in our experiment. In order to be verified by the subsequent experiment, the wavelength of channel one is chosen to be 1549.4 nm; the other channel wavelength is larger than that of channel one, and the wavelength separation is 1.6 nm. Reference [12] has shown that in a short SOA, it is possible to obtain good performance. Therefore, SOA1 will be suitable for cascadability. Because we do not have a short SOA available, in this paper SOA2 is used to verify the precision of our numerical simulation. We consider signals with external intensity modulation (no initial frequency chirp and an initial ER of 15 dB) at 10 Gb/s. Each wavelength transmits a different 64-bit pseudorandom nonreturn-to-zero data pattern. At the receiver, each channel is separated by an optical bandpass filter ($BW = 40$ GHz), followed by a photodiode simulated by a square detector, then passed through an electrical low-pass filter ($BW = 7.5$ GHz) to obtain an eye diagram. Both filters are second-order Butterworth filters [13]. The performance of cascaded gates is estimated by Q-value [1], [14], extinction ratio, and penalty [12]. $Q = 6$ corresponds to a bit error rate (BER) of 10^{-9} [13].

Two kinds of configurations of cascaded SOA gates can be applied in a long-haul WDM system using holding light injection. They are defined as configuration A and B and are shown in Fig. 1(a) and (b), respectively. Configuration A is the same as that used in [15], where one common unmodulated reservoir channel is added. Because the gain of an SOA is different at various wavelengths, the relative value between the signal power ($P_{\rm sig}$) and the holding light power (P_h) is changed after an SOA. In the following numerical simulation, we can see that P_h is very important for a given $P_{\rm sig}$. In configuration B, each SOA gate includes its own holding light generated by a DFB-LD. There are two schemes for holding light injection into the SOA gate: the holding and signal lightwaves copropagate in the SOA gate or the holding and signal lightwaves counterpropagate, as shown in Fig. 1(b). The optical filter is unnecessary in the counterpropagation scheme. In configuration B, P_h at each SOA gate is fixed and not affected by the former SOA gate in a WDM system. In the copropagation scheme, in order to reduce the effect of the holding light on the adjacent SOA gate, an optical notch filter (ONF) is used to suppress the holding light. An optical filter can be used in a single-channel system. We only study the copropagation scheme in our numerical simulation, and we make the following assumptions.

1) ONF has no effect on WDM signals, and the holding light is fully suppressed after the ONF.
2) The gain of the SOA is balanced by a tunable attenuator (TA) following the SOA gates.
3) P_h is smaller than 6 dBm because the gain of the SOA is very small when P_h is large.

III. Experimental Verification

The experimental setup for a single SOA gate is shown in Fig. 2. The multiplexed four-channel WDM signals are modulated at 10 Gb/s with a pseudorandom bitstream (PRBS) of sequence length 2^7-1 chosen to be in agreement with the computer simulations. The signals were decorrelated by 360-ps/nm dispersion compensation fiber. The operating wavelengths are 1549.3 nm (channel 1), 1550.9 nm (channel 2), 1552.5 nm (channel 3), and 1554.1 nm (channel 4). The SOA used in the experiment is 1200 μm long and has less than 0.5 dB of polarization dependence, a confinement factor of 0.6, and a peak gain wavelength of 1550 nm. The SOA saturation

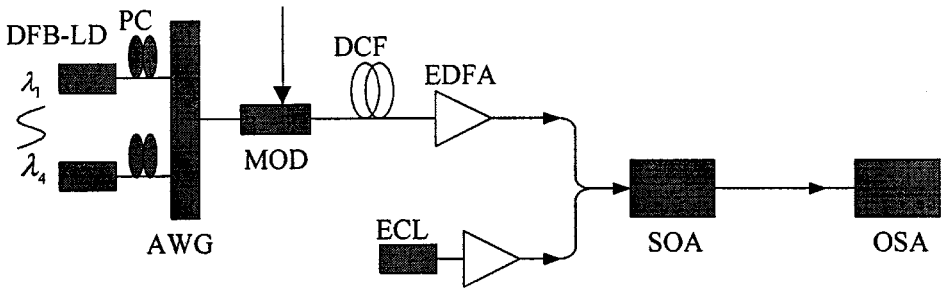

Fig. 2. Experimental setup for a single SOA gate using holding light injection and four WDM signal channels.

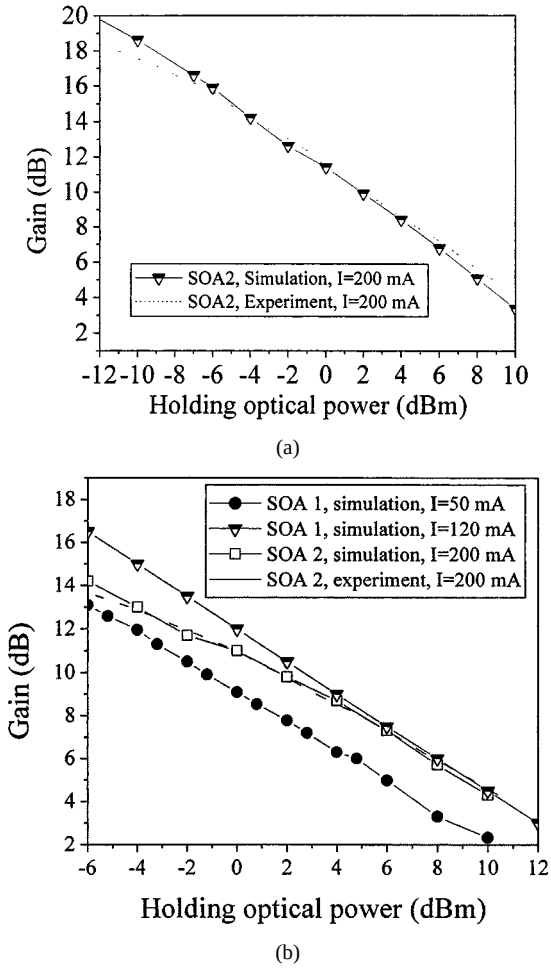

Fig. 3. Measured and numerically simulated gain of channel 2 as a function of holding optical power with signal input power per channel of -12.8 dBm. (a) Single-channel and (b) four-channel system.

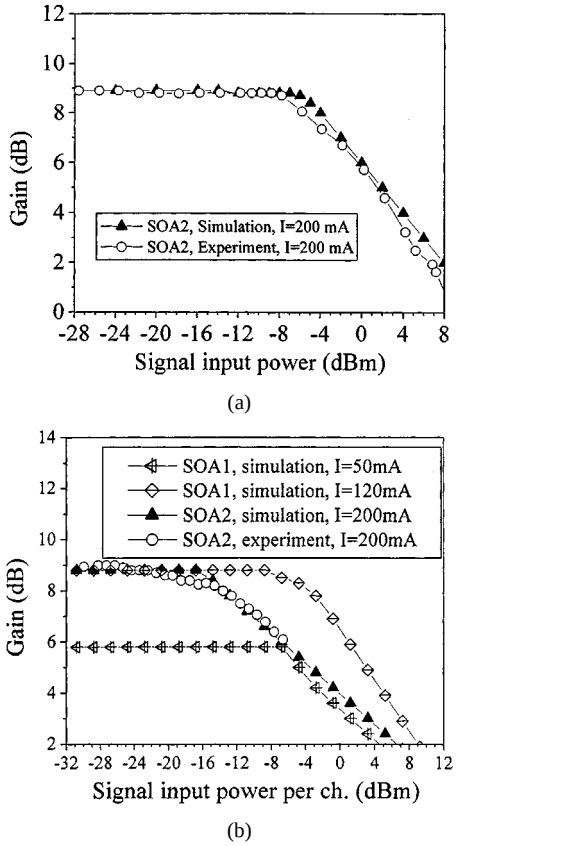

Fig. 4. Measured and numerically simulated gain of channel 2 as a function of signal input power with holding light of 4.6 dBm. (a) Single-channel and (b) four-channel system.

output power is 8.7 dBm, and small signal gain is 25 dB when pumped at 200 mA. Note that the gain and input or output power of the SOA are measured in the fiber, and the fiber-chip coupling less is estimated to 2 dB in this paper. The holding light at 1540 nm and the WDM signals are injected into the SOA by using a 50 : 50% optical coupler.

Keeping the signal average input power per channel ($P_{\rm sig}$) fixed at -12.8 dBm, Fig. 3(a) and (b) shows the gain of channel 2 versus P_h when only channel 2 and when four simultaneous channels operate, respectively. Very good agreement is evident between experiment and theory when both one channel and four channels operate. We can also see that the larger P_h, the smaller the signal gain. Comparing SOA2 operated at 200 mA and SOA 1 operated at 120 mA, the signal gain is almost the same when P_h is larger than 4 dBm.

Keeping P_h fixed at 4.6 dBm, Fig. 4(a) and (b) shows the measured and simulated signal gain versus $P_{\rm sig}$. There is good agreement between experiment and numerical simulation. The measured saturation input powers for SOA2—defined as $P_{\rm sig}$, at which gain is decreased by 3 dB from the unsaturated value—are 0 dBm for single-channel and -6.4 dBm for four-channel operation. So, the saturation input power decreases with increasing number of channels. From Fig. 3(b), we can see that SOA1 has larger saturation input power than SOA2, demonstrating that a short SOA is beneficial for improvement of saturation input power.

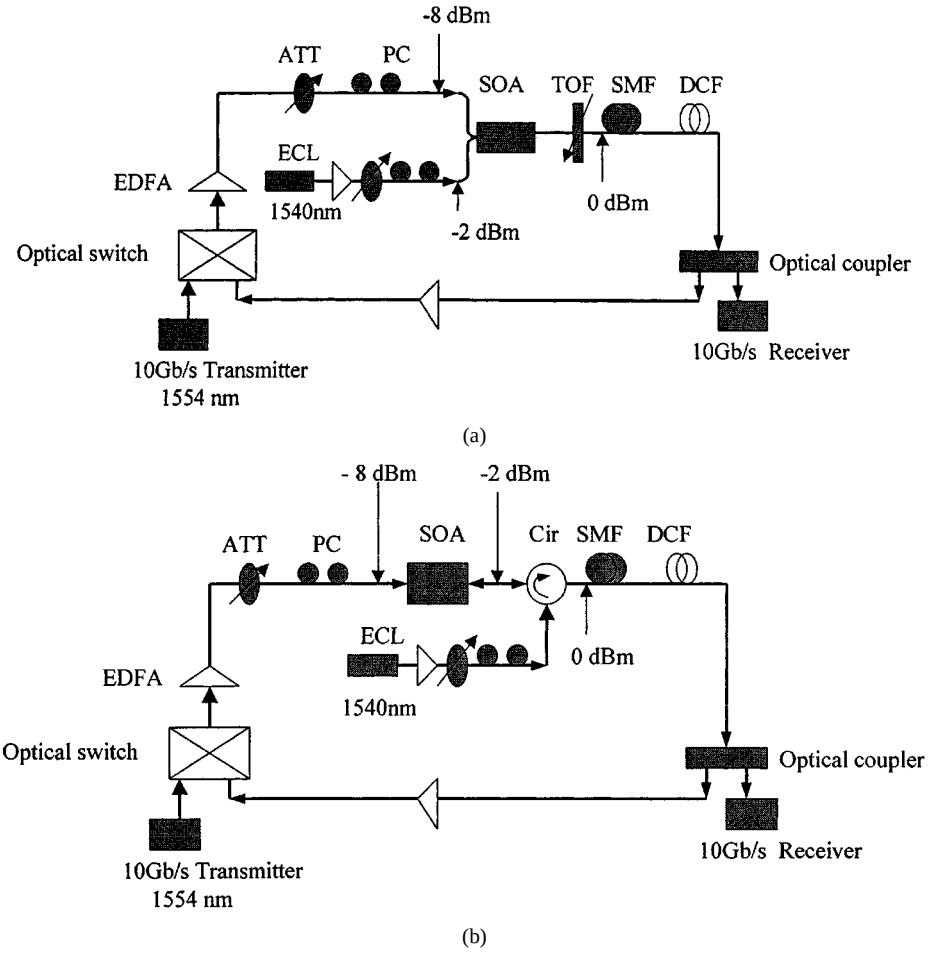

Fig. 5. Experimental setup for multi-SOA gates. (a) Copropagation and (b) counterpropagation.

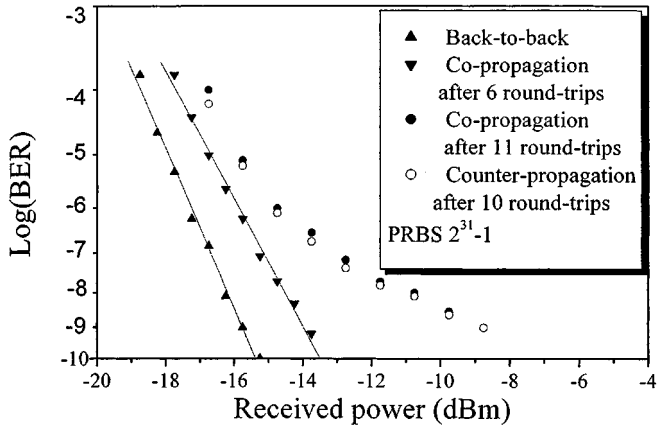

Fig. 6. BER as a function of received power.

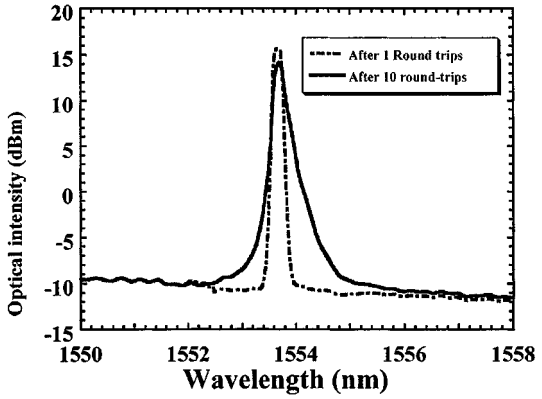

Fig. 7. Optical spectra.

IV. Experiment and Numerical Simulation for Cascaded SOA Gates with Single-Channel Operation

The experimental setup for cascaded SOA gates is shown in Fig. 5. Two SOA gate schemes of copropagation and counterpropagation are investigated and shown in Fig. 5(a) and (b), respectively. The cascadability of the SOA gates is measured in a loop experiment. The SOA used in this experiment is the same as that in Section III. It is clear that our experimental setup is based on configuration B in Fig. 1. The operating wavelengths for signal and holding light are 1554.1 and 1540 nm, respectively. The reflection from the facets of the SOA is smaller than −26 dB. The signal lightwave is modulated at 10 Gb/s with a PRBS of sequence length $2^{31}-1$, and the power of input signal and holding light to the SOA are kept constant for every round-trip. The polarization controllers in the setup are used to keep the interference between signal and reflected signal to a minimum so that the impact of crosstalk from the reflection can be neglected. The loop includes 30-km standard single-mode fiber (SMF) and 6-km dispersion compensation fiber (DCF) providing a full dispersion compensation when the signal wavelength is 1554.1 nm.

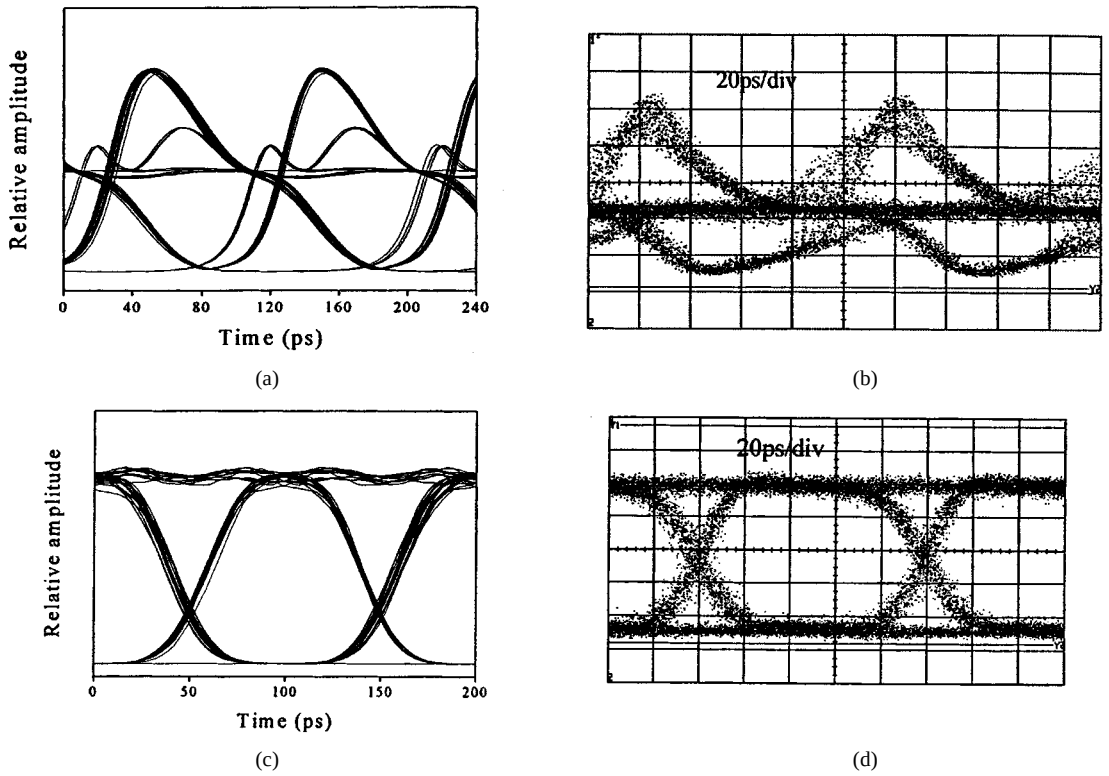

Fig. 8. Eye diagrams after one SOA gate at 10 Gb/s. (a) Numerical simulation after the SOA gate with signal power of -14.8 dBm and without holding light. (b) Experiment after the SOA gate with signal power of -14.8 dBm and without holding light. (c) Numerical simulation with holding power of -2 dBm and signal power of -7.8 dBm. (d) Experiment after the SOA gate with holding light of -2 dBm and signal power of -7.8 dBm.

To reduce nonlinear effects in the fibers, the input powers into SMF and DCF are 0 and -6 dBm, respectively. Using copropagation gating, an optical filter is needed to suppress the holding lightwave; however, using counterpropagation gating, the optical filter is unnecessary, but an optical circulator (Cir) is used in our experiment.

Adjusting the holding and signal lightwave powers into the SOA and using copropagation gating, 11 SOA gates with a BER of 10^{-9} can be obtained when the powers of holding light and signal are -2.7 and -8.5 dBm, respectively. The penalty is 2 dB after six SOA copropagating gating. Using counterpropagation, ten SOA gates with a BER of 10^{-9} can be obtained, and the optimal powers of the holding and signal lightwave are almost the same as those in the copropagation case. Because an optical filter is added after the SOA in the copropagation scheme, SOA ASE noise is suppressed, which leads to the result that one more SOA gate can be cascaded with the copropagation scheme. Signal gain in the SOA is about 14 dB. The BER performance of back-to-back and after cascaded SOA gates is shown in Fig. 6. The error floor appears around 10^{-9}, which means that the maximum number of SOA gates is 11 and 10 for co- and counterpropagation, respectively. These experimental results show that the difference between the co- and counterpropagation schemes is small when the SOA gates are operated at 10Gb/s. The optical spectra of signals in the counterpropagation scheme are shown in Fig. 7. Because of the ASE noise accumulation, the signal optical spectrum after cascaded SOA gates is broadened.

We simulate numerically the above experimental system with the copropagation scheme. Because of computer capacity limitation, we only simulate with a 64-bit pseudorandom nonreturn-to-zero data pattern. Without the holding lightwave, we find that it is impossible to realize $Q > 6$ after two cascaded SOA gates; this is because the SOA has a long cavity and large confinement, which leads to a very strong gain-saturation effect. Fig. 8(a) shows the simulated 10-Gb/s output signal eye diagram after the SOA gate for an input signal power of -14.8 dBm; a clear distortion caused by gain saturation can be seen. Fig. 8(b) shows the experimental result with an input signal power of -14.8 dBm. Fig. 8(c) and (d) shows the eye diagrams of numerical simulation and experiment with holding power of -2 dBm and signal input power of -7.8 dBm after one SOA gate, respectively. No distortion can be seen after the holding light is injected. We can see that the experimental results are in good agreement with the numerical simulations.

Fig. 9(a) and (b) shows simulated eye diagrams for holding light of -2 dBm and no fiber considered. Fig. 9(a) shows that ASE noise accumulation leads to amplitude jitter with signal input power of -7.8 dBm; however, with reference to Fig. 9(b), strong gain saturation effect leads to reduction of the extinction ratio for a signal input power of -2.8 dBm. Fig. 10 shows calculated maximum number of cascaded SOA gates $(Q > 6)$ as a function of signal input power for different holding light powers without fiber. Fig. 10 shows that a large number of SOA gates can be cascaded for relatively large input signal power. When holding light power is -2 dBm, the maximum number of SOA gates is 22 for an input signal power of -6.8 dBm. At low input power levels, the output and the input signals have the same shape; however, the noise accumulation of SOA ASE noise will limit the maximum number of cascaded SOA gates. For large input power, the effect of ASE noise can be reduced, but large

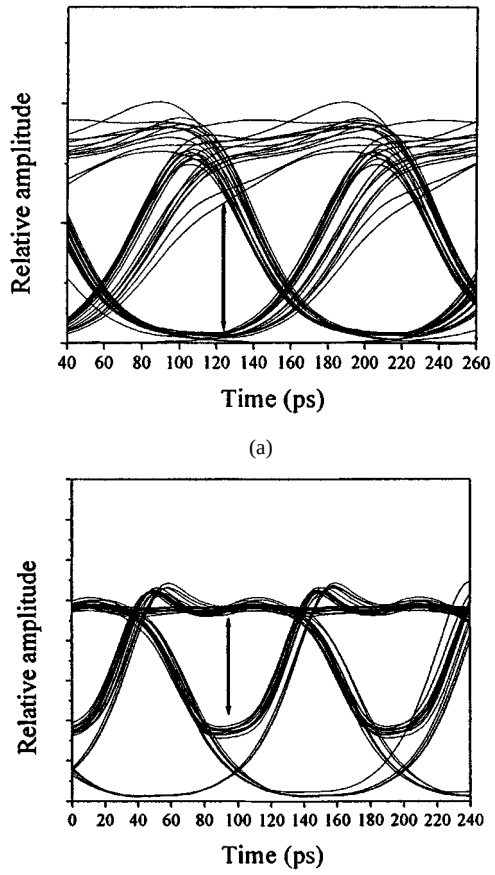

Fig. 9. Eye diagrams with holding light power of -2 dBm and no fiber considered. (a) Signal input power of -7.8 dBm, after 12 round-trips. (b) Signal input power of -2.8 dBm, after ten round-trips.

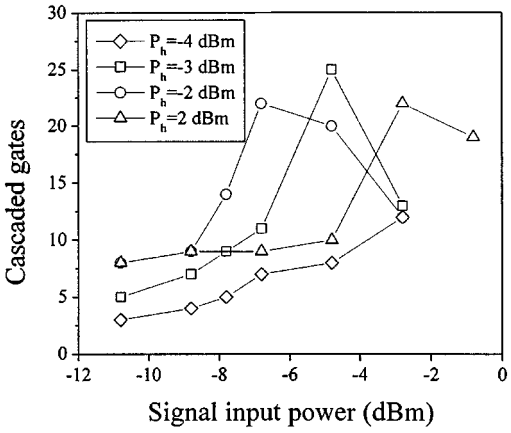

Fig. 10. Calculated maximum number of cascaded SOA gates $(Q > 6)$ as a function of signal input power for different holding light power and without fiber.

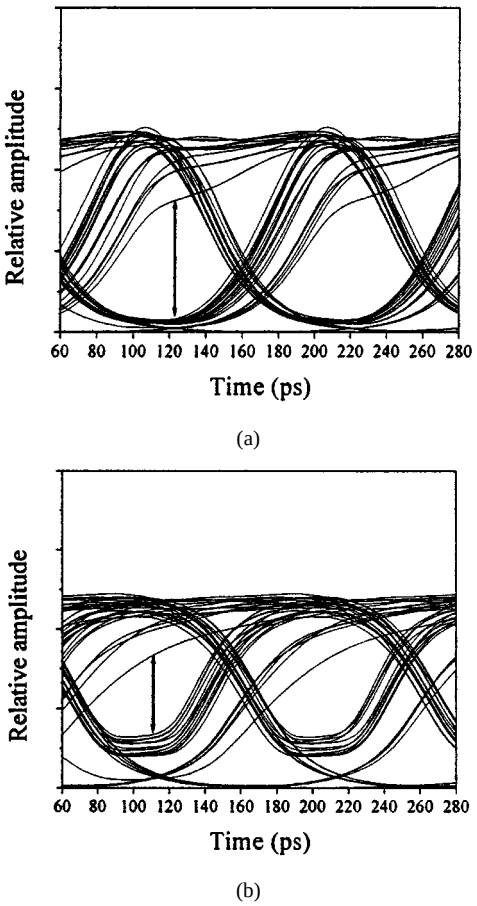

Fig. 11. Eye diagrams with holding light power of -2 dBm. (a) Signal input power of -6.8 dBm, after 20 round-trips and no fiber considered. (b) Signal input power of -6.8 dBm, after 20 round-trips and fiber considered.

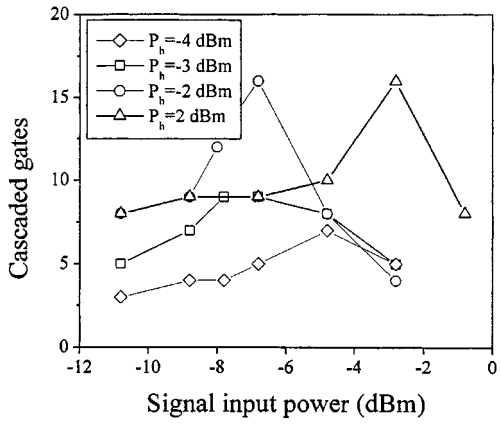

Fig. 12. Calculated maximum number of cascaded SOA gates $(Q > 6)$ as a function of signal input power for different holding light power with fiber.

red-shifted chirp will be generated. The signals with red-shifted chirp will be broadened rapidly when they are transmitted in the SMF. It is well known that the system will need dispersion overcompensation when the input signals have a red-shifted chirp, however, the dispersion is fully compensated in our loop system. This leads to bad transmission performance, which in turn reduces the maximum number of cascaded SOA gates. Fig. 11(a) and (b) shows eye diagrams for holding light power of -2 dBm, signal power of -6.8 dBm, and after 20 round-trips without and with fiber, respectively. We can see that the eye diagram in Fig. 11(b) is worse than that in Fig. 11(a).

Fig. 12 shows calculated maximum number of cascaded SOA gates $(Q > 6)$ as a function of signal input power for different holding light powers with fiber. The fiber characteristics are the same as those in our experiment. The input powers into the SMF and DCF are 0 and -6 dBm, respectively. We can see that the

maximum number of cascaded SOA gates is reduced; this conclusion is in agreement with the above analysis. For small input signal power, the maximum number of cascaded SOA gates with fiber is the same as that without fiber, due to the fact that the output signal for a small input signal power has small chirp. The maximum number of SOA gates is 12 with holding and signal powers of -2 and -8 dBm, respectively. In this case, the results are almost the same as the experimental results for the copropagation scheme. From Fig. 12, we can also see that a maximum number of 16 SOA gates is obtained when the powers of signal and holding light are -6.8 and -2 dBm, respectively. This numerical result is different from our experimental result because the PRBS in our experiment is $2^{31}-1$, which is longer than in our numerical simulation. A longer PRBS will generate larger pattern effect, which pattern effect will be more pronounced at relatively large input signal power. The larger pattern effect will reduce the maximum number of SOA gates. If we use a longer PRBS to simulate the SOA gates, the eye diagram will become worse than in Fig. 9(b). Therefore, it is because of the pattern effect that we cannot obtain the predicted maximum number of SOA gates for an input signal power of -6.8 dBm in our experiment. The experimental results demonstrate that the numerical simulation has its limitation. However, in a WDM system, the distribution probability of "1" and "0" will be equal, which leads to a reduced pattern effect. Therefore, we believe that numerical results for WDM systems will be closer to the experimental results.

V. Numerical Simulation for Multiwavelength SOA Gates

In this section, we simulate multiwavelength SOA gates with a copropagation scheme without fiber. The bit rate is still 10 Gb/s. For a four-channel system, it is clearly seen from Fig. 13(a) that the number of cascaded gates is rather limited when using configuration A, as shown in Fig. 1(a). The main reason is that the ratio between $P_{\rm sig}$ and P_h is changed, which leads to the fact that P_h in the second SOA gate is not the same as in the first one. Fig. 13(b) shows the results by using configuration B, shown in Fig. 1(b). It can be seen that more SOA gates can be cascaded with a short SOA operated at a small injection current; however, in this case, the gain of the SOA is small, which can be seen from Fig. 4(b). Of course, even if P_h is reduced to -1.2 dBm, the number of cascaded gates is still larger than ten, and the gain is larger than 8 dB. Therefore, an SOA with a short length and operated at a small current is suitable for cascading. When $P_{\rm sig}$ is small, the maximum number of cascaded SOA gates is mainly limited by ASE noise accumulation, but too large $P_{\rm sig}$ will lead to XGM of different channels even when holding light is present, so there exists an optimal $P_{\rm sig}$ for a given set of P_h and injection current.

Fixing $P_{\rm sig}$, Fig. 14 shows the number of cascaded gates as a function of P_h. It is clearly seen that there exists an optimal P_h for a given $P_{\rm sig}$. In order to identify what limits the cascadability, Fig. 15(a) and (b) shows Q-value, penalty, ER, and relative power as a function of the number of cascaded gates for SOA1 operated at 120 mA, $P_{\rm sig}=-16.8$ dBm; and for configuration B when P_h is chosen as 4.5, 4, and 3 dBm, respectively.

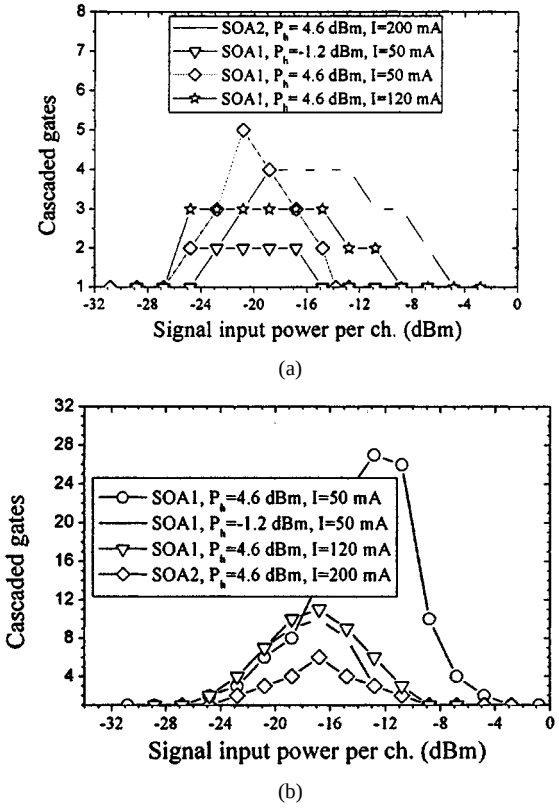

Fig. 13. Number of SOA gates that can be cascaded at $Q > 6$ as a function of signal input power per channel in a four-channel system. (a) Configuration A. (b) Configuration B. Results are from numerical simulation.

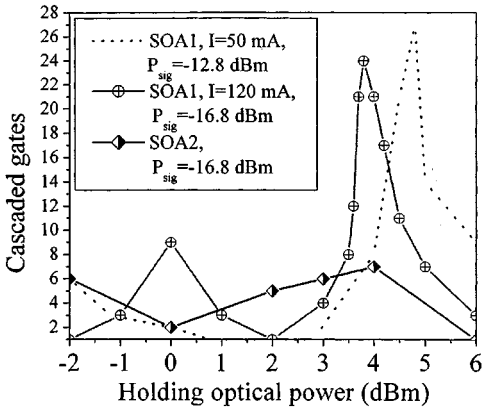

Fig. 14. Number of SOA gates that can be cascaded at $Q > 6$ as a function of holding optical power in a four-channel system with configuration B.

We can see that high ER and high power can be maintained when P_h is chosen as 4.5 dBm. The increased signal power is due to the strong ASE noise power accumulation. The accumulated ASE noise is added to the signal power meaning an increased total power; however, P_h is not changed. Therefore, the accumulated ASE noise will affect the number of cascaded gates. With a P_h value of 4.5 dBm, the maximum number of cascaded SOA gates is 12 at 1-dB penalty. However, if we consider the Q-value, the maximum number of cascaded gates is 23 at BER of 10^{-9} $(Q=6)$. When P_h is chosen as 3 dBm, we can see that the power of the signal is rapidly reduced and becomes close to zero already after transmission over two SOA gates. ER is rapidly reduced after transmission over four SOA gates, and we

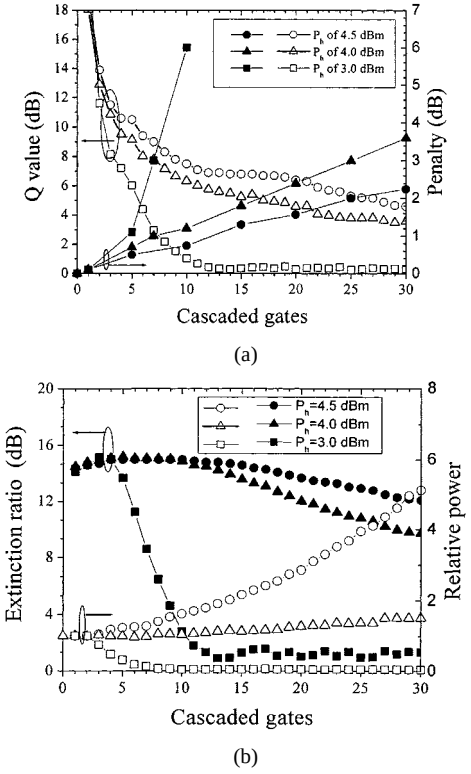

Fig. 15. Q-value, ER, penalty, and relative power of channel 2 as a function of number of cascaded gates in a four-channel system with SOA1 operated at 120 mA, $P_{\rm sig} = -16.8$ dBm, and configuration B. (a) Q-value and penalty and (b) ER and relative power.

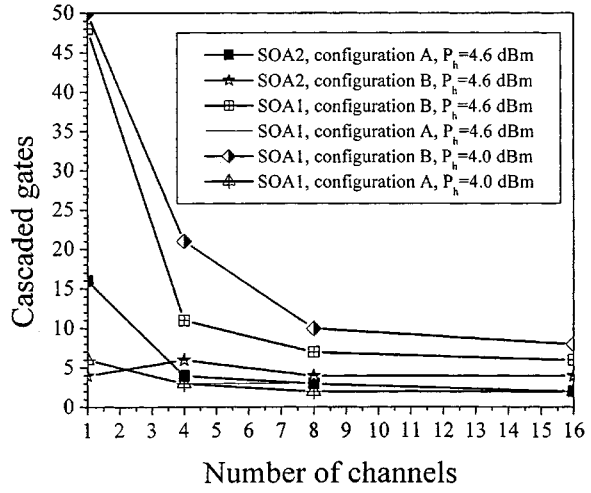

Fig. 16. Maximum number of cascaded gates at $Q > 6$ as a function of the number of channels for an optimal signal input power and SOA1 and SOA2 operated at 120 and 200 mA, respectively. The wavelength of channel 1 is 1549.4 nm; other channel wavelengths are larger than that of channel 1; and the channel spacing is 1.6 nm.

also find that the power and ER of the signal are rapidly reduced even if ASE noise is not taken into account. The rapidly reduced signal power and ER lead to a small number of cascaded SOA gates.

As shown in Fig. 4, the saturation input power per channel is reduced for increased number of channels; this means that the optimal $P_{\rm sig}$ must be decreased in order to limit the XGM of different channels. However, ASE noise accumulation plays a more important role for WDM signals when $P_{\rm sig}$ is small. For this reason, the number of cascaded gates will be reduced with an increasing number of channels. On the other hand, since the bit patterns of the WDM channels are random and independent of each other, the statistics of the signal channels tends to smoothen the total power fluctuations in a system with an increasing number of channels. For that second reason, the XGM will be reduced and a larger $P_{\rm sig}$ can be endured. Therefore, the number of cascaded SOAs will be increased if only the second reason is taken into account. Simultaneously considering the above two reasons, if the second reason is predominant, then the number of cascaded gates will be increased. On the contrary, if the first reason is predominant, then the number of cascaded gates will be reduced. From Fig. 16, comparing a WDM system having eight channels with another having 16 channels, we can see that there is a very small reduction in the number of cascaded SOA gates because of the above-mentioned reasons.

VI. Conclusion

The cascadability of SOA gates when using holding light injection was numerically and experimentally investigated at 10 Gb/s. Our experimental results show that the BER of the signal after two cascaded SOA gates will be larger than 10^{-9} without holding light injection; however, 11 SOA gates can be cascaded with holding light injection. The difference between the co- and counterpropagation SOA gating scheme is small when the SOA is operated at 10 Gb/s; the optical filter can be avoided when counterpropagation is used. Because the red-shifted chirp is generated after SOA gates, the maximum number of cascaded SOA gates will be reduced when the signals are transmitted in a system with full dispersion compensation. Numerical simulations demonstrate that a higher number of SOA gates can be cascaded when the SOA has a short cavity and a small injection current. The holding light power plays a very important role for the cascaded SOA gates: a large number of cascaded SOA gates can be obtained only when a certain holding light power is used.

Acknowledgment

The authors are grateful to Alcatel and Lucent Technologies Denmark for providing the SOA and fibers, respectively. The authors would also like to thank Dr. X. Zheng and Dr. F. Liu for their assistance in part of the experiments.

References

[1] M. Settembre, F. Matera, V. Hagele, I. Gabitov, A. W. Mattheus, and S. K. Turitsyn, "Cascaded optical communication systems with in-line semiconductor optical amplifiers," *J. Lightwave Technol.*, vol. 15, no. 6, pp. 962–967, 1997.

[2] G. Onishchukov, V. Lokhnygin, A. Shipulin, and P. Riedel, "10 Gbit/s transmission over 1500 km with semiconductor optical amplifiers," *Electron. Lett.*, vol. 34, no. 16, pp. 1597–1598, 1998.

[3] D. Wolfson, "Detailed theoretical investigation and comparison of the cascadability of conventional and gain-clamped SOA gates in multi-wavelength optical networks," *IEEE Photon. Technol. Lett.*, vol. 11, no. 11, pp. 1494–1496, 1999.

[4] S. Banerjee, A. K. Srivastava, B. R. Eichenbaum, C. Wolf, Y. Sun, J. W. Sulhoff, and A. R. Chraplyvy, "Polarization multiplexing technique to mitigate WDM cross-talk in SOAs," in *Proc. ECOC'99*, Nice, France, PD3-9, pp. 62–63.

[5] J. Yu, X. Zheng, and P. Jeppesen, "Cascadability improvement of semiconductor optical amplifier based gates using polarization multiplexing technique," *Opt. Commun.*, vol. 178, pp. 309–314, May 15, 2000.
[6] M. Yoshino and K. Inoue, "Improvement of saturation output power in a semiconductor laser amplifier through pumping light injection," *IEEE Photon. Technol. Lett.*, vol. 8, no. 1, pp. 58–59, 1996.
[7] J. Yu, A. Buxens, A. T. Clausen, and P. Jeppesen, "16×10Gb/s WDM bi-directional gating in a semiconductor optical amplifier for optical cross-connects exploiting network connection-symmetry," *IEEE Photon. Technol. Lett.*, vol. 12, no. 6, pp. 702–704, 2000.
[8] J. H. Chen, F. S. Choa, P. S. Cho, J. S. Wey, J. Goldhar, D. L. Butler, and G. L. Burdge, "The gain decompression effect and its applications to very fast wavelength conversions," *IEEE Photon. Technol. Lett.*, vol. 9, no. 6, pp. 755–757, 1997.
[9] A. E. Willner and W. Shich, "Optimal spectral and power parameters for all-optical wavelength shifted: Single stage, fanout, and cascadability," *J. Lightwave Technol.*, vol. 13, pp. 771–781, 1995.
[10] M. Asghari, I. H. White, and R. V. Penty, "Wavelength conversion using semiconductor optical amplifiers," *J. Lightwave Technol.*, vol. 15, no. 7, pp. 1181–1190, 1997.
[11] J. Wang, H. Olesen, and K. E. Stubkjaer, "Recombination, gain and bandwidth characteristics of 1.3 μm semiconductor laser amplifiers," *J. Lightwave Technol.*, vol. 5, no. 1, pp. 184–189, 1987.
[12] B. Bakhshi, P. A. Andrekson, M. Karlsson, and K. Bertilsson, "Soliton interaction penalty reduction by receiver filtering," *IEEE Photon. Technol. Lett.*, vol. 10, no. 7, pp. 1042–1044, 1998.
[13] B. Mikkelsen, T. Durhuus, C. Joergensen, K. E. Stubkjaer, P. Doussiere, G. Garabedian, C. Graver, and D. Leclerc, "High performance semiconductor optical amplifiers as in-line and pre-amplifiers," in *Proc. ECOC'94*, vol. 2, 1994, pp. 710–713.
[14] J. Yu, K. Guan, Z. Xu, and B. Yang, "The effects of different compensation ratios on nonlinear single channel and WDM systems," *Opt. Commun.*, vol. 150, pp. 513–514, 1998.
[15] Y. Sun, A. K. Srivastava, and S. Banerjee *et al.*, "Error-free transmission of 32× 2.5 Gbit/s DWDM channels over 125 km of allWave™ fiber using cascaded in-line semiconductor optical amplifiers," *Electron. Lett.*, vol. 35, no. 21, pp. 1863–1865, 1999.

Jianjun Yu was born in Hunan, China, 1968. He received the B.S. degree in optics from Xiangtan University, China, in 1990 and the M.E. and Ph.D. degrees in optical communications from Beijing University of Posts and Telecommunications, Beijing, China, in 1996 and 1999, respectively.

He joined Research Center COM, Technical University of Denmark, as a Postdoctoral Fellow in June 1999, where he has been engaged in research on high-speed optical communication systems and networks. Since December 1999, he has been an Assistant Research Professor with COM. In February 2001, he joined Agere Systems, Murray Hill, NJ, as a Member of Technical Staff. His current research interests are the generation of WDM short pulse optical source, fiber nonlinear in high-speed WDM/OTDM optical communication systems, all-optical signal procession, wavelength conversion, and the application of semiconductor optical amplifier in optical networks.

Palle Jeppesen (M'69) was born in Vordingborg, Denmark, on August 6, 1941. He received the M.Sc., Ph.D., and Dr. Sc. degrees in electrical engineering from Technical University of Denmark, Lyngby, in 1967, 1970, and 1978, respectively.

During 1968–1969, he was a Research Associate with Cornell University, Ithaca, NY. During 1969–1970, he was a Project Engineer with Cayuga Associates, Ithaca, NY. At both places he did research in the field of GaAs Gunn effect microwave oscillators. From 1970 to 1998, he was successively an Assistant, Associate, Research, and Full Professor at EMI, Technical University of Denmark, first in microwave electronics and then, since 1974, in optical communications. At EMI, he was Head of the Optogroup from 1974 to 1988 and Head of the Center for Broadband Telecommunications from 1988 to 1998. From 1982 to 1984, he also was a part-time Manager of R&D with NKT Elektronik, now Draka Denmark Optical Cable, Lucent Technologies Denmark and Tellabs Denmark. From 1995 to 1998, he coordinated the participation of the Technical University of Denmark in the EU ACTS project METON (Metropolitan Optical Network). Since 1999, he has been a Professor of optical communications at Research Center COM, where he is heading the Systems Competence Area. His current research interests are high-speed WDM optical communication systems, in particular dispersion maps and WDM devices.